Electronic Supplementary Information

ESI Table 1 Summary of the synthetic conditions, initial gel color and gelation time for the preparation of zinc cobaltite aerogels using propylene oxide as gelation agent.

AEROGEL TYPE	Solvent System	Color & Appearance	T_{gel} (h)
P A	acetone	blue; monolithic	5-8
P W	water	light orange solution; white precipitate	no gel
P E	ethanol	reddish purple; highly monolithic	5-8
P P	2-propanol	purple; monolithic	3-6
P M	methanol	light pink solution; white precipitate	no gel
P MP	methanol/2-propanol	reddish pink; highly monolithic	4-6

ESI Table 2 Summary of the synthetic conditions, initial gel color and gelation time for the preparation of zinc cobaltite aerogels using n-butyl glycidyl ether as gelation agent.

AEROGEL TYPE	Solvent System	Color & Appearance	T_{gel} (h)
B A	acetone	light purple; "colloidal-like"	no gel
B W	water	two phases (clear on top, pink on bottom)	no gel
B E	ethanol	rosy pink; very monolithic	3-6
B P	2-propanol	light purple; very monolithic	2-4
B M	methanol	pink; white precipitate, not stable	no gel
B MP	methanol/2-propanol	pink; white precipitate, not stable	no gel

ESI Table 3 Summary of the synthetic conditions, initial gel and gelation time for the preparation of zinc cobaltite aerogels using glycidol as gelation agent.

AEROGEL TYPE	Solvent System	Color & Appearance	T_{gel} (h)
G A	acetone	brown	no gel
G W	water	brown; white precipitate	no gel
G E	ethanol	brown; not stable	6-8
G P	2-propanol	brown; very fragile	2-4
G M	methanol	brown; very fragile	3-5
G MP	methanol/2-propanol	brown; not stable	4-6

ESI Fig. 1 Powder X-ray diffraction patterns of 350°C annealed zinc cobaltite aerogels prepared with propylene oxide (PE and PP) or n-butyl glycidyl ether (BE and BP).

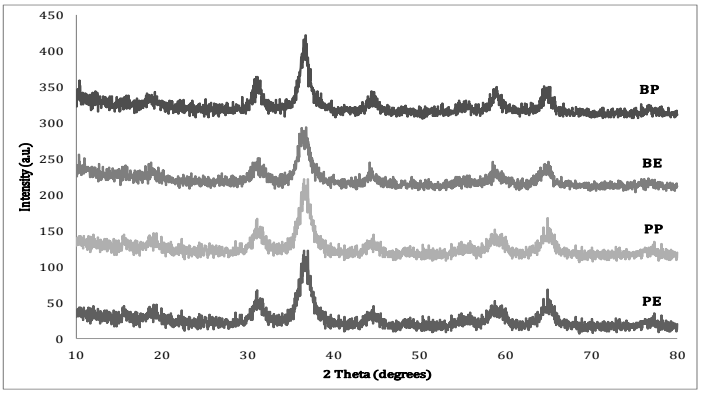

-

ESI Fig. 2 Powder X-ray diffraction patterns of 450°C annealed zinc cobaltite aerogels prepared with propylene oxide (PE and PP) or n-butyl glycidyl ether (BE and BP).

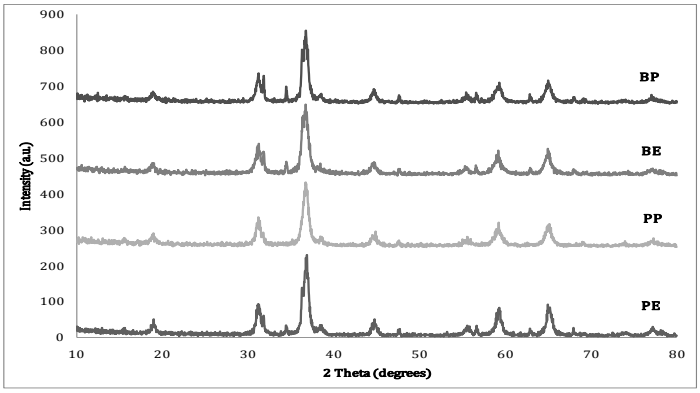

ESI Fig. 3 Cyclic voltammograms of **PE** and **PP** 250°C annealed samples at a 25 mV/s scan rate in 1 M NaOH solution.

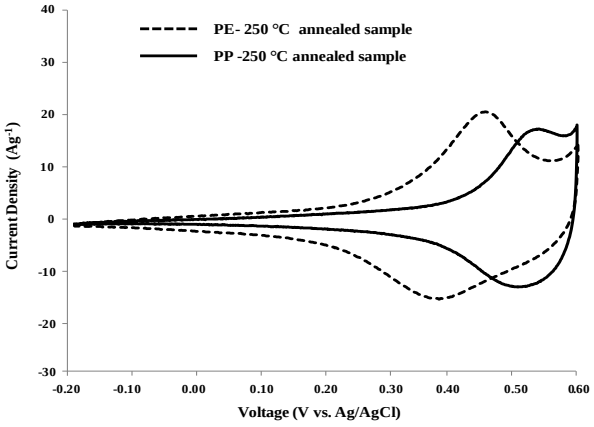

ESI Fig. 4 Decay in specific capacitance with increasing sweep rate of a cyclic voltammetry experiment for the annealed **PE** 250°C sample.

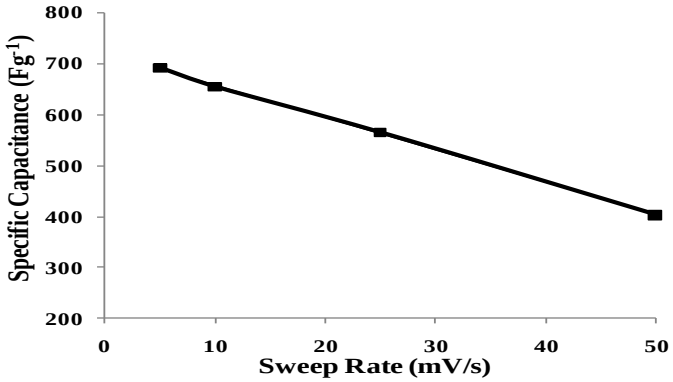

Results and Discussion: Stoichiometric preparation

Powder X-Ray Diffraction. The as prepared aerogel was analyzed by powder x-ray diffraction and shows the sample to be highly amphorous. The crystalline peaks from the as prepared sample could be assigned to several phases. The primary peaks were identified as orthorhombic $Zn(OH)_2$ at 23°, 27°, 29°, 55°, and 58°. Other minor peaks could be identified as belonging to CoOOH. The aerogel was annealed using in situ variable temperature PXRD to determine the temperature at which the desired oxide phase was predominant. As shown in ESI Fig. 5, annealing at 350°C induced the formation of a pure oxide phase corresponding to $ZnCo_2O_4$ (*JCPDS 01-081-2296)*. If annealed at lower temperatures, the result was the formation of a mixed phase composition including both the metal oxide and hydroxide phases.

Annealing at elevated temperatures resulted in an increase in crystallite size as observed by a decrease in the full width at half maximum of the (220) and (311). Analysis of the calcined samples, at 350°C, 400°C, and 450°C show sharp, narrow zinc cobaltite peaks at 2θ (Å)= 31.20 (2.865), 36.76 (2.443), 44.71 (2.026), 55.52 (1.654), 59.21 (1.654), and 65.07 (1.432) corresponding to the (220), (311), (400), (422), (511), and (440) d-spacing facets, respectively. It should also be noted that the presence of Co_3O_4 should not be completely ruled out due to the many overlapping peaks observed from $ZnCo_2O_4$. The other sharp peaks around 40° and 68° are due to the platinum sample holder used.

Once the sample was calcined to higher temperatures (≥350°C), the small peaks correlating to intermediates are diminished. This decrease can be attributed to the physical transformation of these amphorous materials. The high temperature study via powder x-ray diffraction (PXRD) verified that all major phase transitions had occurred around 350°C. With an increase in calcination temperature to 350°C, $ZnCo_2O_4$ dominated the pattern. The diffraction peaks became more sharp and narrow. Again the sample temperature was increased, this time to 450°C, and it was at this temperature that the greatest grain growth was seen and where the product, $ZnCo_2O_4$ became most crystalline.

ESI Fig. 5 PXRD pattern of zinc cobaltite annealed at 350°C, 400°C and 450°C, resepectively (*bottom-to-top*).

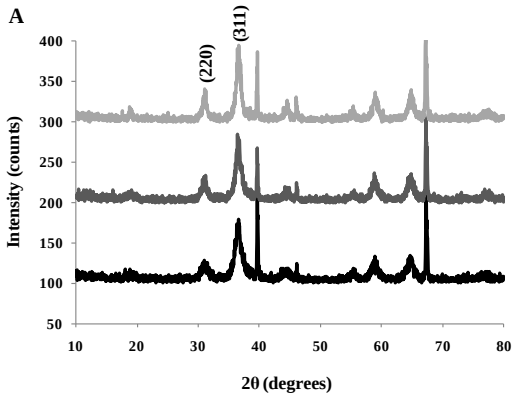

Electron Microscopy. Surface morphology of the as prepared and calcined materials was examined by scanning electron microscopy. These images indicate significant differences in the zinc-cobalt phases. For example, ESI Fig. 6A shows the image of as prepared Zn-Co illustrating a highly interconnected mesoporous network. It appeared to be very fluffy in texture with particles in a "ball-like" structure. Upon annealing the sample to 350°C, a visible change was noticed (see ESI Fig. 6B). Here we noted an increase in both void space and the degree of faceting. With this annealing, it also appeared that the secondary particles became more aggregated. ESI Fig. 6C (zinc cobaltite at 400°C) illustrates that the extended porous character of the aerogel remained upon increased annealing. Here it also appeared that the secondary particles became larger and less well defined. ESI Fig. 6D, highlights the formation of larger clusters having a "spine-like" appearance. One important observation to consider, however, is the change in particle size, which is shown to increase with the higher annealing temperatures, and the network appeared to spread out more. Sintering of the materials typically results in clustering of the materials due to decreasing surface area and grain growth.

The internal microstructure of zinc cobaltite aerogels was investigated in detail by TEM to determine how the particles changed with higher annealing temperatures. Annealing at 350°C, (ESI Fig. 6B inset) shows the material to have very small, spherical particles in a close network. The well, connected network resulted in a relatively high porous network with particles <10nm. In ESI Fig. 6C inset, the particles showed a slight elongation but still appeared relatively well networked in structure with no real change. Finally, in ESI Fig. 6D, a drastic change in the particles was noticed due to extensive grain growth (which correlates to PXRD). Although, most retain their spherical shape; some seemed to lose this distinction and tend to aggregate together.

ESI Fig. 6 SEM image of as prepared and calcined Zn-Co aerogels with corresponding TEM images : (A) as prepared Zn-Co (B) 350°C annealed aerogel (C) 400°C annealed aerogel (D) 450°C annealed aerogel.

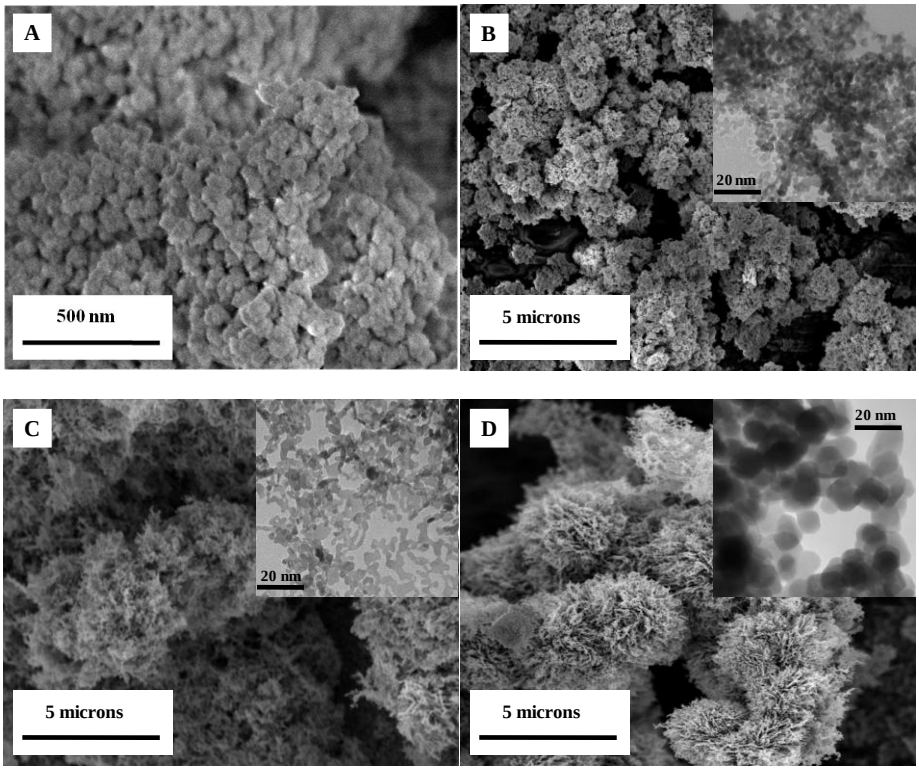

Nitrogen Adsorption/Desorption Analysis. The Brunauer-Emmett-Teller (BET) surface area as well as Barrett-Joyner-Halenda (BJH) pore volume, pore radius, and specific capacitance values are displayed in ESI Table 4. The table displays these tested parameters for as prepared zinc cobalt aerogels as well as calcined samples at 350°C, 400°C, and 450°C.

ESI Table 4 Structural characteristics and specific capacitances of zinc-cobalt aerogels as prepared and annealed at various temperatures.

Annealed Temperature	Surface Area [m^2g^{-1}]	Pore Volume [cm^3g^{-1}]	Pore Radius [nm]	Specific Capacitance [Fg^{-1}]
as prepared	233	0.69	4.23	567
@ 350°C	71	0.19	3.75	515
@400°C	55	0.15	3.67	301
@ 450°C	53	0.11	2.59	212

As expected, the obtained surface area value for the as prepared material is relatively high before annealing. However, after annealing to the oxide form (at the varying calcination temperatures), the surface area, pore volume, and pore radii all decrease significantly for all samples. The decrease in surface area is expected due to the densification of the aerogel structure and grain growth upon annealing at higher temperatures. For the same reason as the decrease in surface area, we can explain the decrease in pore volume. However, the average pore radii values for the as prepared and calcined materials were quite close (all corresponding to mesoporous structures). In addition to the decrease in the structural character of the materials, a decrease in specific capacitance as a function of surface area can also be noted.

Electrochemical Measurements. ESI Fig. 7A-D summarizes the electrochemical capacitance behavior of the $ZnCo_2O_4$ aerogel materials. The capacitance values are tabulated in ESI Table 4. ESI Fig. 7A compares cyclic voltammograms of the as prepared and 350°C annealed aerogel samples. Although the as prepared aerogel has a slightly higher capacitance than the 350°C annealed sample, electrical double layer capacitance is more dominant in the as prepared sample. The greatest contributor to the response of the 350°C, annealed sample is the pseudocapacitance arising from the redox chemistry of the aerogel sample. The pair of peaks near 0.40 V is associated with the $Co(OH)_2$/CoOOH charge transfer processes.

The greater capacitance of the 350°C annealed sample relative to the samples annealed at higher temperatures arises from its smaller particle size (~7 nm), structurally interconnected porous morphology and higher surface area. Moreover, the increase in the pore diameter enhances the diffusivity of electrolyte ions into pores and, in turn, yields high specific capacitances.

In ESI Fig.7B, as expected, while the sweep rate decreases, the obtained specific capacitance tends to increase. ESI Fig.7C and D reveal the cycling performance of the 350°C annealed sample. It was observed that almost 95% of the specific capacitance was retained even after 3000 cycles, and that indicates the materials' outstanding durability.

ESI Fig.7 (A) Cylic voltammograms of as prepared and 350°C annealed sample in 1M NaOH with a 25 mV/s scan rate. (B) Decay in specific capacitance with increasing sweep rate of a cyclic voltammetry experiment for 350°C annealed sample (C) Cyclic voltammograms of 350°C annealed sample 300th cycle and 3000th cycle in 1M NaOH with a 25 mV/s scan rate. (D) Cycling stability test for 350°C annealed sample.